Chemical Engineering Journal xxx (xxxx) xxx

Contents lists available at ScienceDirect

Chemical Engineering Journal

journal homepage: www.elsevier.com/locate/cej

An integrated green methodology for the continuous biological removal and fixation of arsenic from acid wastewater through the GAC-catalyzed As (III) oxidation

Silvia Vega-Hernandez [a], Irene Sanchéz-Andrea [b], Jan Weijma [a,*], Cees J.N. Buisman [a]

[a] Department of Environmental Technology, Wageningen University and Research, the Netherlands
[b] Laboratory of Microbiology, Wageningen University and Research, the Netherlands

ARTICLE INFO

Keywords:
Acidianus, Activated carbon
Airlift Reactor, Arsenite oxidation
Scorodite

ABSTRACT

Herein we report the findings of an integrated green process for the continuous oxidation and biomineralization of the most toxic As(III) from acidic streams using a laboratory-scale airlift bioreactor operated at thermoacidophilic conditions and fed with Fe(II) as electron donor. As(III) oxidation catalyzed by granular activated carbon (GAC), biological Fe(II) oxidation and scorodite crystallization took place simultaneously in the reactor, allowing the treatment of influent solutions containing 0.65 $g{\cdot}L^{-1}$ As(III). At a hydraulic retention time of 2.2 days, a stable arsenite oxidation efficiency of 99% was achieved, while the removal of total arsenic was 93%. Scorodite was yielded as the main solid product whose physical characteristics such as average size (250 μm) and the developed crystalline structure allowed the easy harvesting from the reactor and reflected the high stability by the low arsenic release of 0.4 $mg{\cdot}L^{-1}$ after 60 days of leaching. The analysis of the microbial composition in the reactor suspension and the precipitates indicated the dominance of thermoacidophilic archaeon of the genus *Acidianus*. Similarly, the attachment of microorganisms to the precipitates observed by scanning electron microscopy, suggested that the precipitation in our system was biologically mediated. The simultaneous arsenic oxidation and removal through catalyzed oxidation and biological processes provide the basis for a new and cost effective green methodology for arsenic fixation from acid As(III)-containing wastewaters.

1. Introduction

Arsenic (As) is an ubiquitous natural element in the earth's crust [1] and a hazardous contaminant commonly generated from the processing of base metal ores. Health effects due to exposure to As species are severe and include skin and lung cancer, neurological effects, hypertension and cardiovascular diseases [2]. Accordingly, the World Health Organization has set a very low standard of 10 ppb for drinking water. To protect the environment and drinking water resources, hydrometallurgical process streams containing arsenic concentrations (mainly As(III)) in the range 500–10000 ppm [3,4] must be treated prior to the reuse of the water in the process or the disposal of the treated effluent in tailings facilities [1]. The removal and stabilization of this toxic element still is a significant and continuous challenge for the non-ferrous extractive metallurgical industry. Traditional methods to remove arsenic from industrial wastewaters and metallurgical operations include lime neutralization and chemical co-precipitation of arsenate with ferric iron [5]. Recent technologies, including adsorption/desorption, encapsulation, electrocoagulation have been developed and are widely applied to treat As-containing streams. However, the main disadvantage is the cost of such processes, the high iron dose needed and the amount of unstable generated waste [6,7].

The precipitation of arsenic and iron as scorodite ($FeAsO_4{\cdot}H_2O$) is regarded as the preferred route for arsenic fixation due to the high arsenic content, high stability, low iron consumption and good settling properties of the product [8,9]. Different methods for chemical precipitation of scorodite, mainly from As(V) solutions, under hydrothermal and atmospheric conditions have been described [5,10]. Similarly, under ambient conditions, the precipitation of biogenic scorodite from As(V) solutions was demonstrated [4,11–13]. In the biogenic process, the saturation control is given by the biological oxidation of Fe(II) leading to the synthesis of crystalline scorodite at 70 °C in the absence of primary seeds.

The oxidation state of arsenic is of importance for the design of

* Corresponding author.
E-mail address: jan.weijma@wur.nl (J. Weijma).

https://doi.org/10.1016/j.cej.2020.127758
Received 10 August 2020; Received in revised form 5 November 2020; Accepted 15 November 2020
Available online 20 November 2020
1385-8947/

effective removal strategies. Arsenite (As(III)) is 60 times more toxic and mobile than arsenate (As(V)) and is commonly released to the weak acid process waters produced by mineral processing [1,14,15]. Thus, in order to optimize the removal of arsenic and stability of the precipitates, a primary oxidation step is required. Available studies on As(III)-oxidation in acid streams (pH < 1.5) are limited. At these conditions, arsenite oxidizing activity has been scarcely reported, and at low rates for thermophilic iron-oxidizing species of the genera *Sulfolobus* and *Acidianus* [4,13,16–20], which still represents a drawback for the scale-up and development of the biological process. On the other hand, hydrogen peroxide has proven to be efficient oxidant of As(III) used in the industry [21], However, one of the main disadvantages besides the high cost of the oxidant is its instability as it decomposes in contact with solids. Alternatively, the catalytic oxidation of As(III) in acidic solutions by activated carbon in the presence of oxygen at ambient conditions has been reported [22]. With this concept, oxidation efficiencies up to 99% were reported using catalyst ratio between 1/17–1/30.

Earlier reports developed by our group demonstrated that the spontaneous As(III) oxidation by granular activated carbon (GAC) combined with the biological Fe(II) oxidation led to the precipitation of biogenic scorodite in batch experiments [23,24],providing a promising green strategy for the removal of arsenic from acidic wastewaters. Following the concept of saturation control without the addition of neutralizing chemicals, the optimization, and characterization of the scorodite precipitates were also studied in different media with and without GAC catalyst [24]. Preliminary results showed that a higher removal of arsenic and the formation of settleable scorodite particles were obtained at a lower catalyst concentration, confirming the role of the catalyst in As(III) oxidation and suggested the induced mineralization as the primary mechanism of crystallization as a result of controlled biological Fe(II) oxidation in As(III)-rich solutions.

For further scale up and use in metallurgical industry, the development of a continuous process will be essential. Herein, we aim to develop such a continuous process for precipitation of biogenic scorodite in an airlift reactor fed with simulated As(III) and Fe(II) containing acidic solutions. The scorodite produced in the continuous bench-scale reactor was examined for its chemical composition and long-term stability through the toxicity leaching test procedure.

2. Materials and methods

2.1. Mixed culture and growth media.

Enrichment cultures of thermoacidophilic iron-oxidizing archaeon [23,24] were used as inoculum in this study.

The reactor was inoculated with 10% v/v of the thermoacidophilic mixed culture pre-grown in medium containing 0.5 g L^{-1} Fe(II) and 0.5 g L^{-1} As(III) at a pH of 1.3 and 70 °C. Cell numbers were monitored during the experiment through cell counting using a Burker chamber (Germany). The synthetic feeding medium, ferrous iron stock and arsenite solutions were prepared as described previously [23].

The granular activated carbon (NORIT GAC 830 W) used in the experiments was sieved to particle sizes between 0.8 and 1.4 mm and washed with sulphuric acid (1 M) followed by rinsing with deionized water in order to remove impurities. It proved that in the bench scale reactor, larger particles were difficult to suspend at the applied gas flow rates. Characteristics of the used GAC are described elsewhere [23].

2.2. Airlift reactor set-up and operation.

An internal loop airlift reactor with 9 L of working volume was used in this work. The riser had a length of 0.60 m and a diameter of 0.07 m. With a reactor diameter of 0.13 m, the riser/downcomer area ratio was 0.44. The reactor temperature was controlled at 70 ± 2 °C with a heating bath (Julabo F25, Germany). The pH was controlled at 1.2 ± 0.1 using H_2SO_4 (5 M) and NaOH (5 M) solutions. Air and oxygen were supplied to the reactor giving an inlet concentration of 27.5% O_2 in the mixed gas. Therefore, the feed gas flow rate was controlled by separate mass flow controllers (Brooks thermal mass flow meter, type 5850 E, 0–60 L h^{-1}). The gas was recycled at 60 L h^{-1}, with a membrane pump (KNF N828) providing a superficial air velocity in the riser of 0.59 m s^{-1}. The water vapor in the bleed air was condensed with a reflux condenser connected to a cooling bath (Julabo F25, Germany) and the condensate was returned by gravity to the reactor. The reactor was operated without external recirculation of liquid or solids.

Redox potential (Eh, mV) and pH were measured with glass electrodes (QR480X-Pt billed-triple junction (vs. Ag/AgCl in saturated KCl) and QP181X-triple junction, respectively; Prosense, the Netherlands). Slope calibration of the pH electrode was done with pH 1 and 4 buffers. Dissolved oxygen was measured using an oxygen dipping probe DPPSt3 (Presens, Germany) connected to a Fibox-3 fiber optic oxygen transmitter (Presens, Germany. The oxygen sensor was calibrated at 0% with nitrogen and at 100% with water-saturated air.

The airlift reactor consisted of three consecutive experimental stages. (I), a start-up phase of batch mode for 12 days, (II) day 13–33, continuous mode with a hydraulic retention time (HRT) of 3.1 days, and (III) day 34–98, continuous mode with an HRT of 2.2 days The influent media composition varied between batch and continuous operation. In stage I (batch operation), about 1 g of Fe(II) L^{-1} and 1 g of As(III) L^{-1} were added to the reactor solution giving a molar ratio Fe/As of 1.29. When the reactor was switched to continuous operation (stage II and III), the concentrations were reduced to 0.63 g of Fe(II) L^{-1} and 0.65 g of As (III) L^{-1} (Fe/As: 1.3). No external seed crystal were added to the bioreactor.

Samples of the liquid influent and effluent were collected regularly for chemical analysis. The composite samples were filtered through 0.45 μm acetate membrane filters (VWR syringe filters). The filtrated solids fraction from the effluent samples and dried in a vacuum oven at room temperature before solids characterization.

2.3. Methods

2.3.1. Iron and arsenic analysis

The dissolved Fe and As species of the filtered liquid samples as well as the Fe/As ratio of synthesized precipitates were determined as described previously [23].

2.3.2. Characterization of the precipitates

In order to determine the physicochemical properties of the generated precipitates, solid samples were withdrawn from the reactor. Characterization included particle size distribution (PSD) analysis, XRD, FT-IR, TGA and SEM-EDX, out as described previously [24].

2.3.3. Toxicity characteristic leaching procedure

Arsenic leaching from the biogenic precipitates was determined following the standard Toxicity Characteristic Leaching Procedure (TCLP) of EPA [25]. Serum bottles (150 mL) containing acetate buffer at pH 4.95 as leaching medium and at a fixed solid: liquid ratio of 20% w/w. The bottles were shaken at 20 °C. Samples were taken after 20 h, 7 days and 60 days and sampling volume was replaced with fresh acetate medium.

2.3.4. Microbial community analysis

In order to assess the microbial composition, two different samples were withdrawn from the reactor and processed for DNA extraction. On one hand, 5 mL of the bulk solution were centrifuged at 13,400 *g* for 10 min, supernatant was discarded, and the pellet was resuspended in 250 μL of sterile Milli-Q water, this sample was termed “Biomass”. On the other hand, 1 g of the mineral fraction was washed with Milli-Q water; this sample was termed “Solid”. DNA was extracted in triplicates with the FastDNA Spin Kit for Soil (MP Biomedicals, OH) according to manufacturer’s protocol. DNA was then cleaned with the Zymo DNA Clean &

Concentrator kit (Zymo Research, CA). PCR was performed as described elsewhere [26]. The demultiplexed Illumina Hiseq reads of the 16S rRNA gene amplicon sequencing were deposited at the European Nucleotide Archive (ENA) under study PRJEB32058 in fastq format with accession numbers ERX3291747- ERX3291752.

A multiple alignment of the sequences was performed using Muscle v3.7 [27] with the default parameters. This multiple alignment was used to create an approximate maximum- likelihood tree using FastTree v2.1.8. [28] with default parameters. The tree was visualized with iTOL [29]. For the identity network, using the multiple sequence alignment created for the phylogenetic tree, a pairwise distance was calculated using Clustal Omega – 1.2.3 [30] for all detected 16 rRNA sequences and threshold was settled at 0.9 for the clustering. Network visualizations were constructed using Cytoscape (v. 3.7.1) [31]

2.4. Calculation of the Ion activity product

The Ion Activity Product (IAP) of the reactants of scorodite was calculated based on Eq.1 as described elsewhere [12]

$$FeAsO_4\hat{A}\cdot 2H_2O(\text{Scorodite}) \leftrightarrow Fe^{3+} + AsO_4^{3-} + 2H_2O \quad (1)$$

3. Results and discussion

3.1. Arsenite and ferrous iron oxidation efficiency in ALR

The airlift reactor was operated in batch mode during the first 12 days at an initial pH 1.2 ± 0.1 with GAC (4 g·L^{-1}) using starting concentrations of 1 g·L^{-1} As(III) and 1 g·L^{-1} Fe(II), resulting in a molar ratio Fe/As of 1.29. As(III) oxidation started immediately and 42% of As(III) was depleted within one day (Fig. 1A). Overall As(III) and Fe(II) oxidation during stage I amounted to 83% and 76%, respectively (Fig. 1A,C). Simultaneous with arsenite oxidation and Fe(II) oxidation, precipitation of dissolved As took place (Fig. 1A). Iron and arsenic precipitated during the first 8 days at an approximate ratio Fe/As: of 1.3, however, between day 8 and 12 this ratio increased to 4 (Fig. 3A), owing to the precipitation of secondary iron phases. This was coupled to a change in the pH of the solution, which increased to 1.4 at day 9 and to the increase of the redox potential from +0.35 to +0.43 mV. (Fig. 2).

On day 13 the reactor was switched to continuous operation with an HRT of 3.1 days, based on prior batch results obtained with the same GAC concentration [24] and, with an influent medium containing 0.65 g·L^{-1} As(III) and 0.63 g·L^{-1} Fe(II). The pH fluctuated between 1.18 and 1.24, which was strictly controlled during continuous operation. Eventually, the precipitated Fe/As molar ratio decreased, and from day 17 until the end of the experiment, the formation of secondary amorphous phases was no longer observed. The precipitation of poorly crystalline phases is unwanted in the process. However, two routes determining the fate of these phases has been considered to take place in the crystallization process, first the solubilization in the acid media or secondly, its conversion into crystalline phases [32–34] of which, the first one is the most likely to occur. The formation of amorphous phases may influence directly or indirectly the precipitation of scorodite [34]. Of the oxidized Fe, only 40% was precipitated, while 45% of As precipitated, achieving an average removal of 0.24 ± 0.08 g·L^{-1} d^{-1} of Fe and 0.28 ± 0.04 g·L^{-1} d^{-1} As (Fig. 1B and 1D). The precipitation in stage II apparently was limited by the oxidation of As(III) which fluctuated between 50 and 60%. The molar Fe/As precipitation rate ranged between 0.9 and 1.4 in stage II (Fig. 3A) and the absence of visible precipitates in the effluent indicated that precipitates were effectively retained in the reactor.

The decrease of the HRT to 2.2 days at day 31 marked the start of stage III. At the same time, the oxygen flow rate was increased to 4.7 L·h^{-1} and the recycle gas flow was switched to 100 L^{-1}h^{-1}, giving a dissolved oxygen concentration in the reactor of 4.0 ± 0.1 mg O_2 L^{-1}.

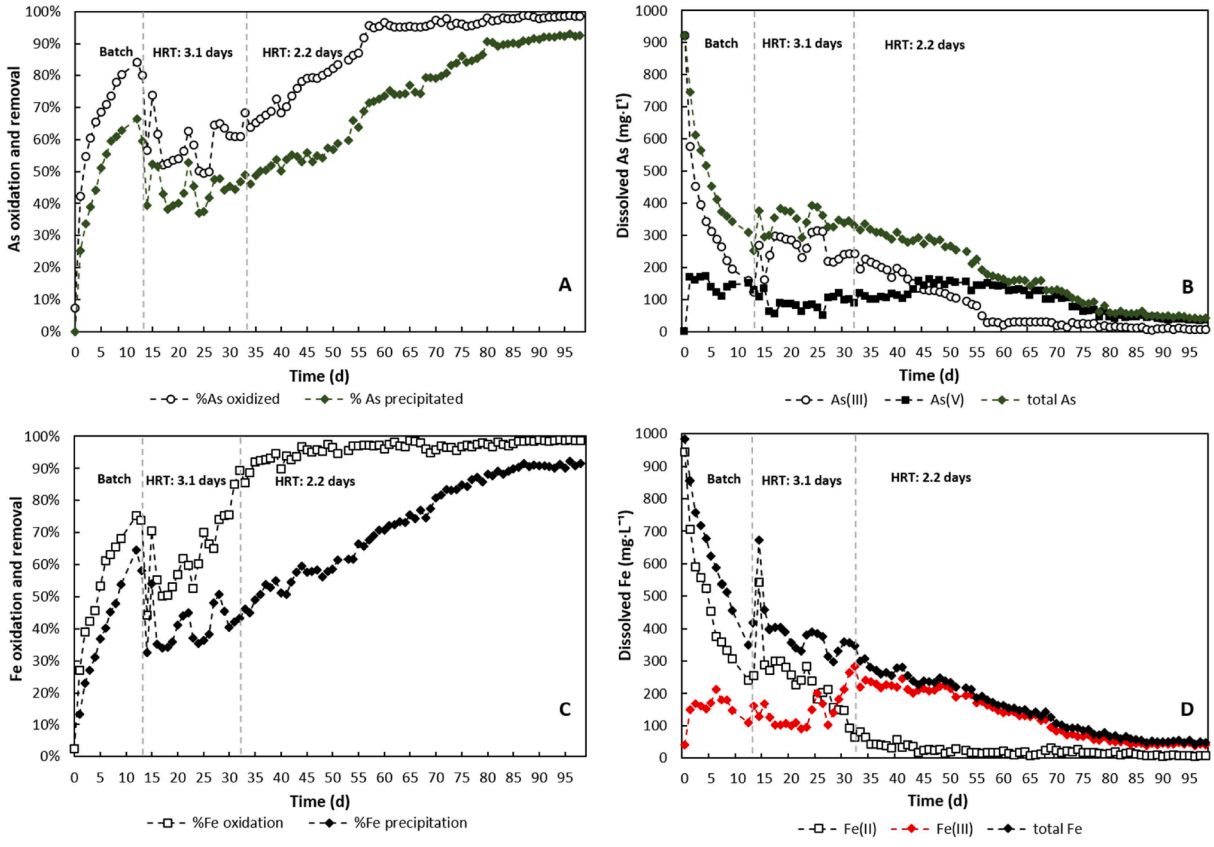

Fig. 1. Overall arsenic and iron oxidation and removal in the airlift reactor operated at 70 °C during batch and continuous operation (from day 13 onwards). A: As (III) oxidation and removal efficiency B: dissolved As species, C: Fe(II) oxidation and removal efficiency, D: dissolved Fe species.

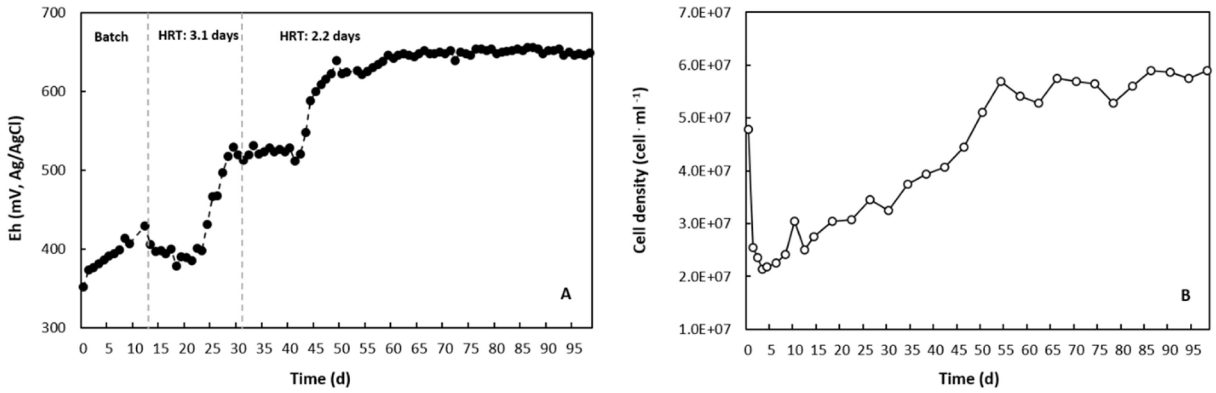

Fig. 2. Redox potential (mV, Pt vs. Ag/AgCl in saturated KCl) and microbial growth measured as cell density (cell·ml^{-1}) in the airlift reactor.

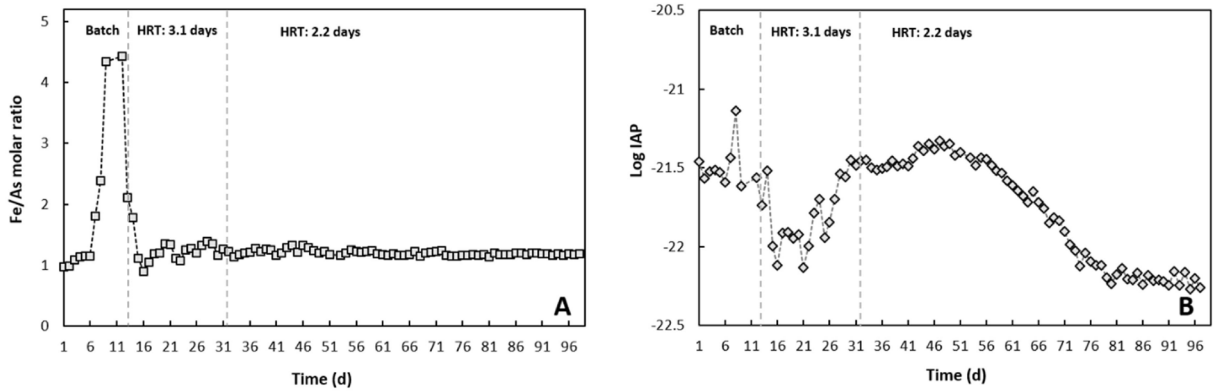

Fig. 3. Fe/As molar ratio of Fe and As species removed from solution (A) and calculated Ion activity product (Log IAP) of the produced biological scorodite.

The increased recycle flow resulted in the effective lifting and better distribution of the activated carbon granules, which had partially settled to the reactor bottom in stage II. The arsenite oxidation increased during stage III until a stable situation was observed from day 58 until the end of the experiment (day 98). An average oxidation rate of 0.641 g·L^{-1} d^{-1} of As(III) was found, corresponding to an oxidation efficiency of 99%.

In the case of ferrous iron conversion, the rates were not markedly influenced by the improved mixing of the granules in the reactor. The oxidation efficiency increased with around 16% during the last phase of continuous operation and a plateau was reached after day 50 with approximately 98.4% of the Fe(II) oxidized (Fig. 1D). This was reflected also in the ORP which reached a maximum of + 0.65 mV during this phase. As shown in Fig. 2, the increment of ORP due to the increased ferrous oxidation was also coupled to the growth of the iron oxidizing mixed culture, expressed by the increased quantity of planktonic cells during batch and continuous operation.

Once the oxidation and precipitation rates improved in stage III of reactor operation, the concentration of total dissolved iron and arsenic concentrations considerably decreased to an average of 0.047 ± 0.01 g·L^{-1}; of which, As(III) and Fe(II) were low, ranging around 0.01 g·L^{-1}. During stage III the reactor content turned to light green, typical for scorodite (Figure S3). The concentration of dissolved arsenic and iron in the effluent solution was also monitored (Figure S4) resulting in similar concentrations of total iron and arsenic around 0.04 ± 0.018 g·L^{-1}. The concentration of As is too high to allow for direct discharge. Thus, a post treatment like co-precipitation with ferrihydrite will be needed in practice.

Oxidation of As(III) is essential in the process of arsenic immobilization however, this alone does`not ensure the effective removal of arsenic from solution. It must the follow either by adsorption or the precipitation. Traditionally the fixation of arsenic from relative dilute arsenic streams is accomplished by the co-precipitation of the oxidized As(V) with Fe(III) and neutralization, which results in a mixture of amorphous arsenical ferrihydrite with molar Fe/As ratio of 3–5 and thus substantial amounts of waste (i.e., arsenate bearing ferrihydrite plus gypsum). The biological production of scorodite, controlled by bio-oxidation reactions has been previously demonstrated to produce a compact precipitate resembling the (natural) mineral [35] and with a low Fe:As close to 1. This implys a much lower Fe consumption and a lower volume of the solid waste residue. The drawback of both methods lies firstly, in the predominance of the most toxic As(III) in hydrometallurgical processes, which requires a prior step of oxidation and secondly, in increased capital cost associated with the necessary chemicals and equipment. Chemical processes include oxidation and precipitation, where each process is carried out in separate operational units. Furthermore, with the use of stronger oxidants such as hydrogen peroxide, permanganate, or ozone, is effective but expensive [36]. In contrast, biological As(III) oxidation coupled to the simultaneous Fe(II) oxidation and concomitant scorodite precipitation has been reported in a single system; however, in low volume batch bottles as vessel reaction [4,20].

Bearing this in mind, in the present study we proposed a combined biological process where As(III) oxidation, catalyzed by granular activated carbon, a cheap catalyst, Fe(II) bio-oxidation, and the biogenic scorodite precipitation continuously take place in a single reactor. Hence, the energy input and the environmental footprint are reduced. One of the benefits of the proposed biochemical process is not only the in-situ production of oxidant and the induced precipitation, which avoids the addition of chemicals but also the production of a compact precipitate with good settling properties. Our results provide a better-insight into the possible applicability of the process to higher volumes of simulated streams and the long-term stability of the crystals produced.

Likewise, the use of an airlift reactor as a single process operating system offers more advantages compared to separate units than only the prevented investment cost for the separate As(III) oxidation reactor. For example, the airlift reactor is effective for mass transfer of oxygen by recycling the effluent gas, providing sufficient oxygen for both arsenite and ferrous iron oxidation. Less equipment is needed in the single stage process, e.g., less pumps, mass/gas flow controllers, sensors etc. The airlift is an also well-mixed system and was suitable to keep both scorodite crystals and GAC particles suspended, without attrition of the GAC particles. Furthermore, it has been shown that the use of air-lift reactors is beneficial for crystallization processes with respect to crystal growth [37]. Airlift and gas-lift bioreactors are already applied on a full scale for over 20 years, also in metallurgical operations and can be considered proven technology [38,39]. For application of the biological scorodite process, the airlift reactor design may need some modification for collection and separation of the scorodite solids. Incorporation of a settling in the reactor of a settling compartment designed could represent a suitable to remove particles above a cut-off sedimentation rate (or particle size). After day 59 until the end of the experiment, the ORP was very stable at +649 ± 4 mV. This coincided with high oxidation efficiencies for As(III) and Fe(II) (Fig. 1), a high As(V):As(III) molar ratio (Figure S6) and a low Fe(II) concentration (Figure S7). The ORP may represent a suitable parameter for monitoring process performance and as a control parameter, for instance to adjust the HRT.

3.2. Arsenic precipitation

The saturation of the solution was evaluated using the ion activity product (IAP) of ferric arsenate. Scorodite mostly precipitated in the reactor at log IAP values from −21.5 to −22.3 (Fig. 3). The IAP decreased at the start of continuous operation (stage II) due to decreasing As(V) concentrations. However, the IAP increased immediately after the arsenite oxidation rate improved, resulting in increased As(V) activity in solution, without additional changes between day 31 until day 61 of stage III where the As(III) oxidation rate reached 95.3%. Until the end of the experiment (day 98) total As precipitation rate increased to 93% and IAP values fluctuated around −22 ± 0.5 being in the range of IAP values previously reported during scorodite precipitation [8,12,23].

The evolution of the particle size distribution of precipitates from the reactor is shown in Fig. 4A. The average particle size was 19 μm on day 9 (stage I, batch mode). Also, particles < 1 μm were found in the sample and at the start of continuous operation (day 18) which might be attributed to the amorphous ferric arsenate solid phase formed during stage I. During continuous operation, the precipitates grew from an average particle size of 43 μm in stage II to 230 μm at the end of stage III. The growth of the crystals over the continuous operation indicated that crystal growth dominated over nucleation. The bioscorodite precipitates showed good settling properties and the complete deposition of 0.5 $g \cdot L^{-1}$ of solids with particle size between 15 and 300 μm was achieved in 5 min at settling velocities between 1 and 228 $m \cdot h^{-1}$ in a 500 mL glass cylinder (Fig. 4B).

The continuous precipitation of biogenic scorodite in the airlift reactor led to the growth of crystals aggregates which were identified as: (1) a fraction that remained in suspension facilitating the precipitation of scorodite on the existing particles instead of the reactor walls and (2) solids settled to the bottom of the reactor, which was beneficial for the collection of the solids from the solution.

3.3. Structural characterization of the precipitates

Precipitation of iron and arsenic took place during the entire experiment as revealed by the decrease of soluble total Fe and As in solution, and by the appearance of a solid phase on day 9 of batch operation. On day 12, samples taken from the reactor visually revealed two solid phases, a compact material of light green color and a gelatinous-like phase. The former settled at the bottom of the reactor while the gelatinous material was observed in suspension and the bottom of the reactor (from which it was taken for analysis).

The X-ray diffraction analysis of the both samples revealed the presence of scorodite as the main mineral phase of compact greenish precipitates (Figure S2A) and the formation of a short-lived gelatinous fraction identified as an amorphous iron arsenate phase (Figure S2B). Thus, in agreement with the estimated Fe/As ratio precipitated, the formation of other iron precipitates than scorodite was induced. Comparable XRD patterns have been obtained during arsenate adsorption studies to ferric oxides conducted at similar temperature (75 °C) conditions by Jia, Xu, Wang and Demopoulos [40] and with molar Fe/As ≥ 2. We found similar XRD pattern for ferric iron precipitates (Figure S2D) together with the scorodite precipitates from stage II (although to a lesser extent), that were no longer visible during stage III (Fig. 5).

The greenish precipitates collected during stage II were also identified as scorodite (Figure S2B). While broad peaks of lower intensity where observed in the sample from stage I (Figure S2A), the sharper and narrower peaks observed in samples of stage II and stage III (Fig. 5) are indicative of larger crystal size and increased crystallinity (degree of structural order) [41,42].

The dominance of scorodite crystalline phases in the precipitates collected at the end of stage III was confirmed by the complete match of the sharp peaks to the diffraction patterns of mineral scorodite and by the high intensity counts (Fig. 5A). The overall weight loss by TGA was 15.8%, close to the theoretical water content of mineral scorodite (15.6%). FT-IR analysis of the precipitates showed the characteristic peak for arsenate bending (V1 AsO_4^{3-}) at 820 cm^{-1} [43]. Besides, 2 peaks were also observed at 1008 and 1030 cm^{-1} which might be related to the incorporation of sulphate, possibly from the washing step of the samples prior the characterization as documented by Gonzalez-Contreras, Weijma and Buisman [44]. The strong water stretch and bonding was

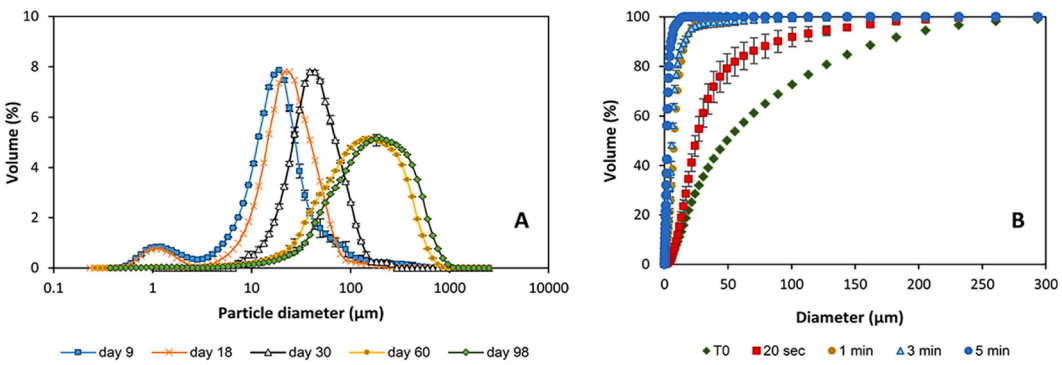

Fig. 4. PSD analysis of the produced bioscorodite precipitates (A) and the solids volumetric settling velocity as function of diameter according to Stoke's law (B) with their respective standard deviation (n = 3).

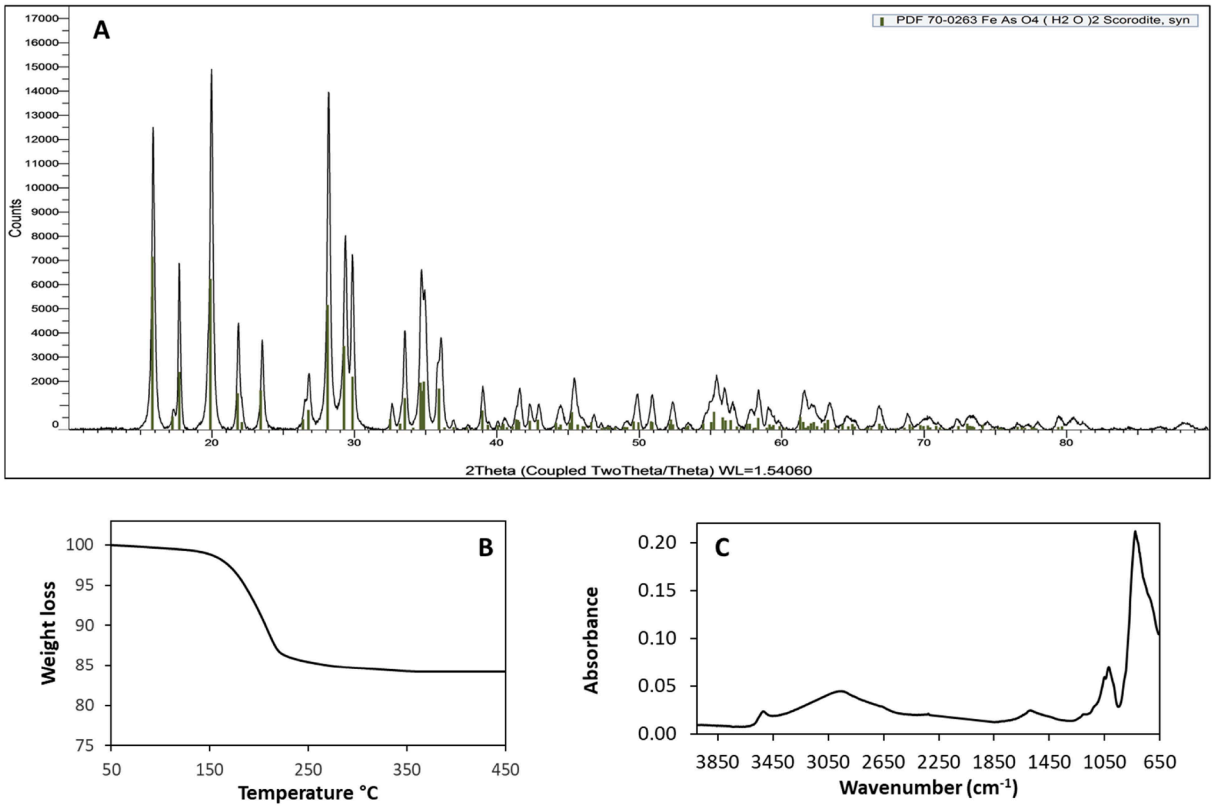

Fig. 5. Structural characterization of bioscorodite crystals collected at the end of the continuous experiment. (A) XRD analysis of the precipitates. (B) TGA analysis showing the structural water content between 170 °C and 240 °C. (C) FTIR spectra of precipitates.

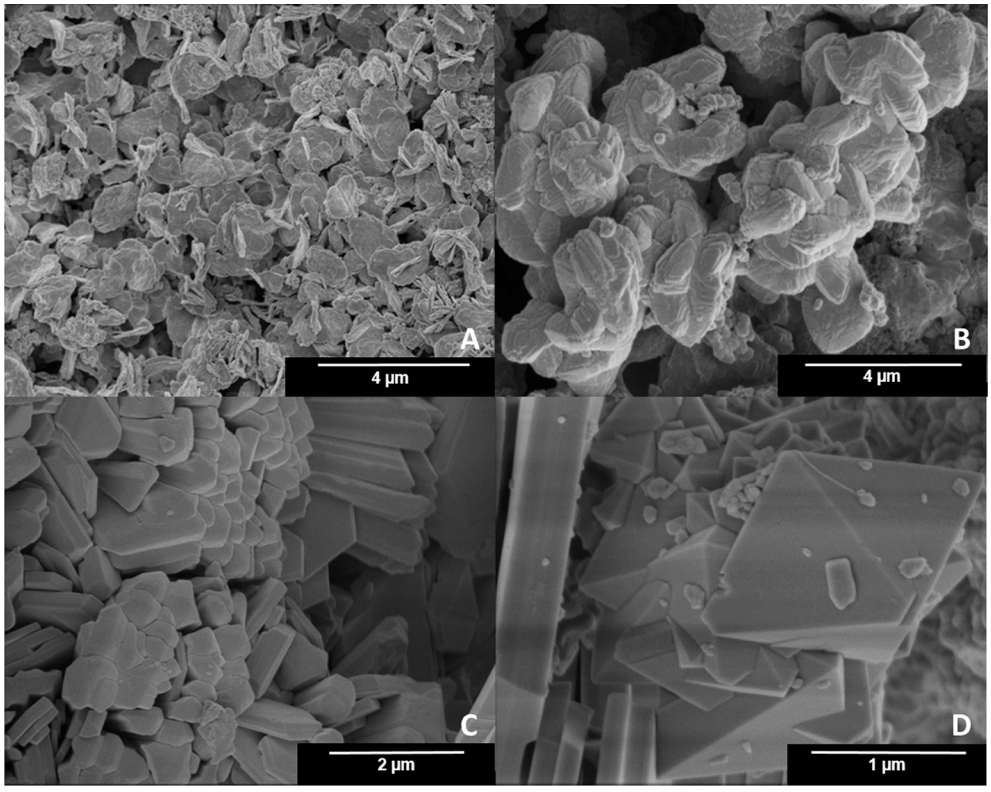

Fig. 6. Scanning electron microscopy (SEM) of the precipitates collected during stage II at day 17 (A) and 27 (B) and during stage III at day 55 (C) and day 81 (D) of continuous operation from airlift reactor.

identified in the region of at 1600 and 2960 cm^{-1}.

The morphology of the bioscorodite particles was examined by scanning electron microscopy (SEM). The results displayed in Fig. 6 indicated that the precipitated scorodite developed from an irregular to a more crystalline shape. The solids observed at beginning of stage II consisted of agglomerates with irregular structure containing crystallites of 0.5 μm, in agreement with the particle size distribution analysis. The development of more crystalline particles was visualized in the solid aggregates at day 27 (Fig. 6B). By the end of stage III, clusters of crystals and individual scorodite particles with octahedral structure were observed (Fig. 6C and 6D).

As already found with the PSD analysis, precipitates collected at the end of the experiment consisted on agglomerates with sizes up to 300 μm. The analysis of the surface of these bigger particles revealed that these consist of well-ordered planes of dipyramidal form with an estimated size of 1–2 μm (Fig. 7). This characteristic growth has been reported previously for crystalline scorodite [45] and referred as habit I by Gonzalez-Contreras, Weijma, Weijden and Buisman [12].

The elemental composition of the precipitates was also analyzed by SEM-EDX (Figure S5), showing that Fe/As molar ratio ranged between 1.1 and 1.25 for the precipitates taken at day 25 and 57. The elemental composition of the precipitates collected at the end of the continuous experiment slightly changed and an average Fe/As content of 1.04 was found. The SEM-EDX analysis furthermore revealed the presence of P and S in small proportion of 1.6%wt and 0.66%wt, respectively in the solid sample. The presence of 8.21%wt C and 1.67%wt N may result from the association of microorganisms with the precipitates.

3.4. Arsenic leaching from the biogenic scorodite precipitates

Determining the release of arsenic into solution is of environmental significance to assess if the formed precipitates are a safe medium for long term arsenic storage. The leaching of arsenic from the precipitates collected during stage I-III was evaluated by the toxicity characteristic leaching procedure (TCLP) (Fig. 8).

Arsenic leaching values for all the samples was below the permissible EPA limit of 5 $mg{\cdot}L^{-1}$ of As. As shown in Fig. 8, the precipitates collected during stage I (day 12) leached around 2.05 $mg{\cdot}L^{-1}$ As after 20 h which decreased to 1.4 $mg{\cdot}L^{-1}$ after 60 days. Precipitates from stage II and III initially leached 1.5 and 0.6 $mg{\cdot}L^{-1}$ of As, respectively (20 h), which decreased to 1.2 and 0.46 ± 0.01 $mg{\cdot}L^{-1}$ after 60 days. The higher leaching values of solids from stage I may well be due to the presence of less stable amorphous material (observed on the XRD) [9,35,46]. Leachability of arsenic has been associated to the crystallinity and aging time [44,45,47,48], which could explain the lower leaching of solids from stage III compared to stage II.

3.5. Microbe-mineral association and microbial composition in airlift reactor

In reactor samples from stage II and stage III, coccoid and bacillus shaped microorganisms associated with EPS-like structures and solids were observed by SEM (Fig. 9A and B). The dominance of rod-shaped cells with surfaces that appeared to be also damaged was observed in reactor suspension (Fig. 9C). The association of microorganisms with the minerals supports our previous finding that the cells play a key role in scorodite precipitation[23], not only by providing the reactant ferric iron by ferrous iron oxidation, but also by acting as secondary nuclei. EPS formation has been reported for thermoacidophilic species of *Acidianus, Sulfolobus* and *Metallosphaera*, and it is suggested that EPS provides protection against environmental stress such as low pH [49]. The association of cells with solids also might facilitate biomass retention in the reactor.

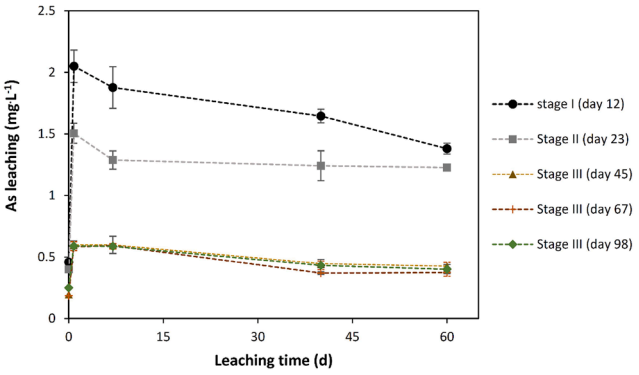

Fig. 8. Arsenic leaching from precipitates produced during batch and continuous operation under TCLP test. Error bars show the mean (±) standard deviation of the triplicates.

The analysis of the microbial community composition in the reactor was done by 16S rRNA sequencing of samples from the bulk solution and the solids, designated as "Biomass" and "Solid" respectively. Both samples were collected at the end of the experiment. After filtering low abundance OTUs (below 0.01%), the microbiome composition of both biomass and solids showed a relative low diversity comprising 61 OTUs in total, belonging to 24 different genera (Fig. 10A and B). In the biomass sample, that was comprising the planktonic cells in the reactor, the 61 OTUs were identified, however in the solids sample only 21 OTUs were detected (Fig. 10A and B).

In thermophilic bioleaching processes iron/sulfur oxidizing mixed cultures are commonly employed from which no more than three species often dominate in continuous-flow operations [50] even though under thermoacidophilic conditions (<60 °C) reactions are mainly performed by archaea and only a smaller number of other bacterial species may be present [51].

Members of the *Sulfolobaceae* family (most of them annotated as *Acidianus* spp.) were the most abundant microorganisms detected in the 16S rRNA survey in both Biomass and Solid samples representing the 45.9 and 92.3% of the total microbial community (Fig. 10A and B). As aforementioned, members of this genus, such as *Acidianus brierleyi* have

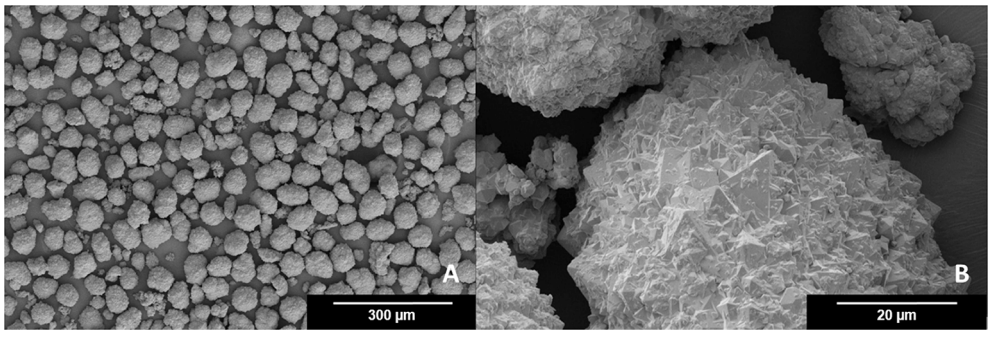

Fig. 7. SEM analysis of the scorodite crystals collected at the end of the experiment and surface characteristics.

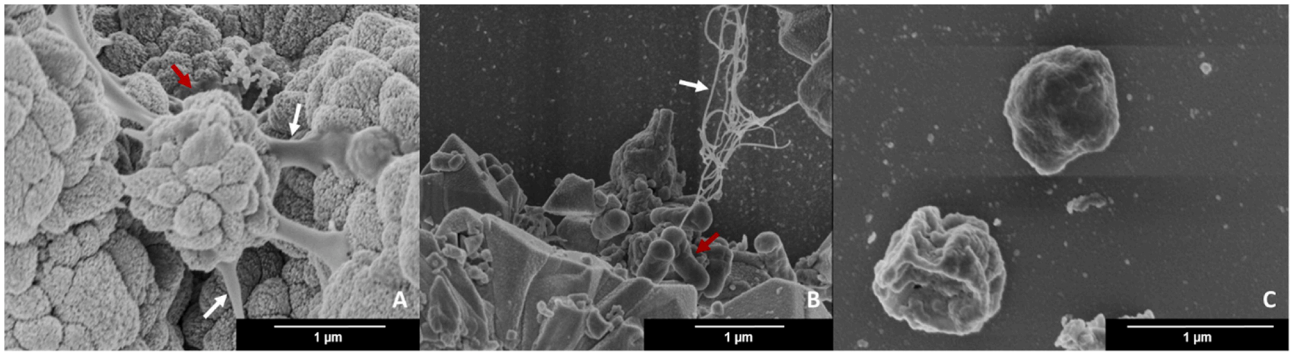

Fig. 9. SEM images of the precipitates from stage II and III indicating the presence of EPS like-structures (white arrows) and coccoid-like and bacillus shaped cells adhered to the solids (red arrows) (A and B) and microorganisms from reactor suspension (C).

been linked to the simultaneous ferrous iron, arsenite oxidation and to the concomitant scorodite precipitation [4,16,20,52]. Similar to the iron oxidizing archaea *A. sulfidivorans*, *Metallosphaera sedula* and *sulfolobus* spp. which has been reported to mediate scorodite precipitation but in the less toxic As(V) solutions [11,12,53]. Phylogenetic distance analysis (Fig. 10C) of the sequences from the reactor samples showed that Firmicutes, Crenarchaeota and Proteobacteria were the three main phyla clustering at 90% similarity. Furthermore, using the reference strains *Acidianus* spp. and *Sulfolobus* spp. revealed that the OTU29, highly abundant and dynamic in the Biomass and Solid samples, is clustering very close to the *S. metalicus, A. brierleyi, A. sulfidivorans* and *S. tokodaii*. Although *A. brierleyi* and *S. metallicus* were known to be part of the inoculum, further studies need to be performed to determine more precisely the taxonomic composition of this specialized community.

Beside *Acidianus* spp. the second most abundant taxa was *Ralstonia* spp. accounting for 9 and 4.8% of the total reads in the Biomass and Solid samples, respectively. Members of *Ralstonia* have been found in mine tailing sediments and associated with the oxidation of As(III) [54,55]. Other genera, such as *Geobacillus*-related sequences also showed a high abundance, but with markedly difference within the planktonic biomass and the solid phase (9.2 and 0.5%, respectively). *Geobacillus* spp. are thermophilic, aerobes with a chemi-organotroph metabolism, also reported in mine ecosystems [56]. Other iron oxidizing species such as *Sulfobacilllus* were found in the bulk solution. In spite of the low abundance (approximately 1–2% in the biomass sample), this microbe is known to be part of the mixed culture inoculated in the reactor at the beginning of the experiment. Although the optimum growth temperature of this specie (40–60 °C) is below the tested conditions, the adaptation of these species to adverse even deleterious conditions has been previously reported in thermoacidophilic leaching systems and geothermal sites [51,57]. Moreover, the interaction of *Sulfobacillus* species, e.g., *S. thermosulfidooxidans* and *Acidianus* species have been reported to be beneficial for the dissolution of minerals [58]. Therefore, the role of this microorganism in the oxidation and/or precipitation cannot be excluded.

Overcoming the negative impact that a higher concentration of As (III) can have on the microbial Fe(II) oxidizing activity while keeping a stable As(III) oxidation in the system is critical for the development of a robust biological process. To achieve this purpose, some strategies for the process optimization and enhancement of the biological Fe(II) oxidation rate in the system can be further considered, including:

1) HRT optimization: as one of the most critical parameters of a continuous operation that might result in a lower capital-cost of the unit process. A follow-up study should determine the minimum HRT where near complete oxidation of the influent ferrous iron can be sustained while avoiding microbial washout from the system. Te The present study indicates the feasibility of lowering even more the HRT (to 1 day) iwth similar oxidation efficiency.
2) Selection and adaptation of a favorable mixed culture: if we aim to increase the initial concentration of arsenic in the system as well as the extent of the scorodite precipitation, apart from Fe(II) bio-oxidation performance, improving the biomass concentration is crucial. Although at the start of the experiments, the negative effect of As(III) was significant in the biological oxidation of Fe(II), the prolonged exposure might have resulted in the adaptation of the microbes as observed in the increased cell density. UsingUsing other carbon sources might also contribute to the microbial growth of thermoacidophilic microbes at the studied conditions.
3) Study the addition of alternative iron substrates: the ability of thermoacidophilic microorganisms to leach minerals such as pyrite at high rates could make it a suitable iron source and a low-cost option for the bioscorodite process. Furthermore, the growth of archaeal species through the bioleaching of the above-mentioned mineral has been previously reported, indicating the beneficial influence of inorganic iron and sulfur as secondary energy substrates [59,60].

4. Conclusions

The catalyzed oxidation of arsenite by activated carbon in combination with the iron oxidizing mixed culture led to the formation of scorodite as the main product in the studied continuous airlift reactor system at pH 1.2 and 70 °C. The mixing of the activated carbon granules with the bulk solution is crucial to ensure the complete oxidation of arsenite in the system. I In the reactor the oxidation of iron is controlled by the activity of the mixed culture, which was reflected by the increased cell concentration and the gradual increase of the iron oxidation rate, probably due to the reduced toxic effect of As(III). Under these extreme conditions mainly archaeal populations were enriched in the reactor system. The high percentage of archaeal species obtained by the molecular analysis and the visualized structure EPS like-structures suggest that the formation of scorodite is indirectly mediated by the microbial surface or surface components (exopolymers). The biogenic scorodite produced showed similar characteristics to mineral scorodite, which as revealed by the water content and the low arsenic leachability during the extended leaching test. Furthermore, the quality of obtained sludge facilitated the retention of the particles in the system, which offers significant advantages such as: (1) avoided scaling in the reactor (2) increased density of the sludge and (3) easy solid–liquid separation, which allows getting a suitable material for disposal.

The obtained results provide an important step forward to the potential applicability of the process to higher volumes of acid As-streams as well as for the development of a sustainable and integrated approach for waste management and improvement of water quality for recycling or discharge. This in turn will contribute to reducing the environmental footprint of the mining industry.

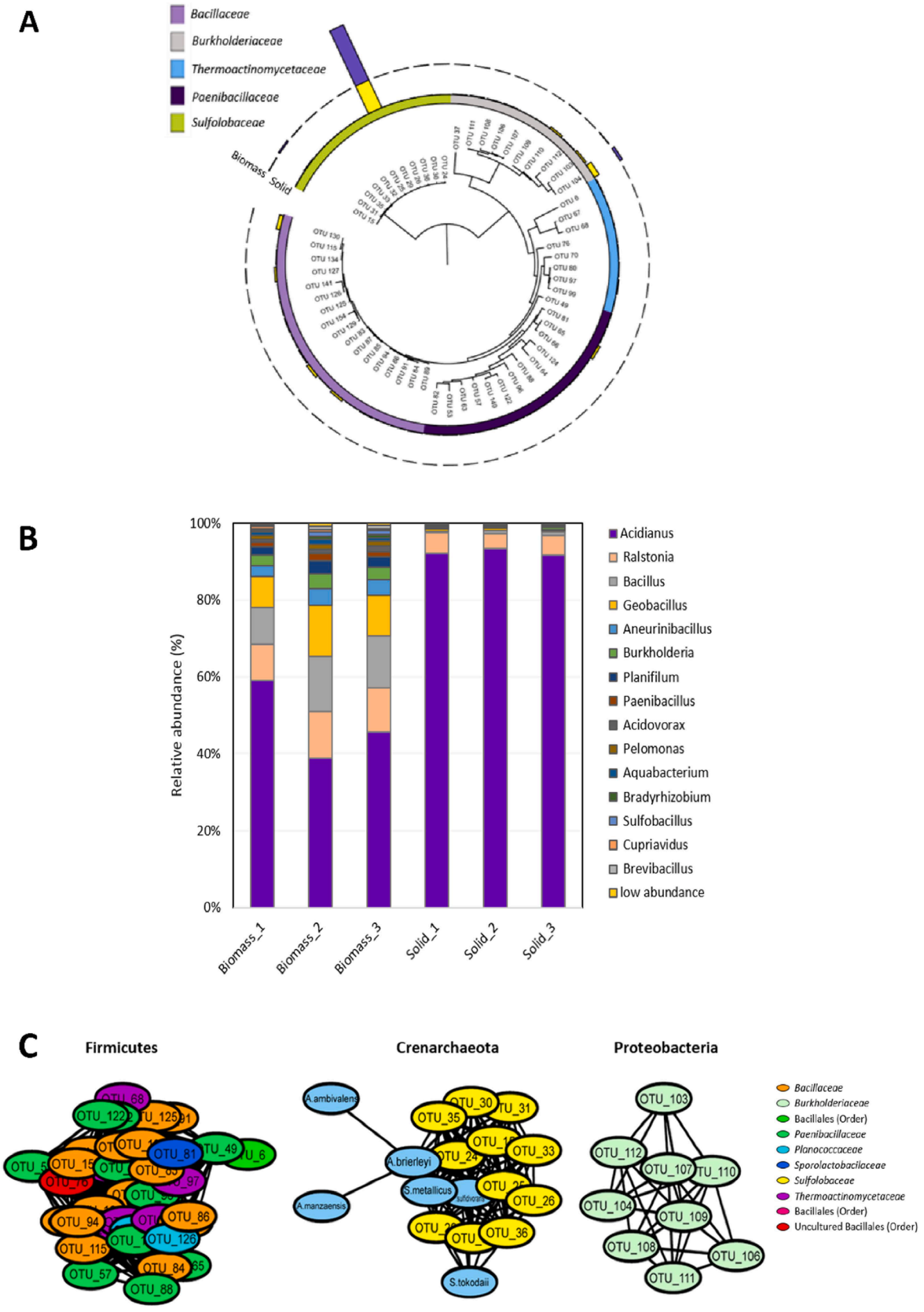

Fig. 10. Reactor (liquid) samples and scorodite precipitates microbiome (named as Biomass and Solid respectively). (A) Reactor microbiome phylogenetic tree of the detected OTUs (n = 61) based on 16S RNA gene. Taxonomic classification, at Family level, is indicated by the colors in the inner circle. Outer circles represent the relative abundance of detected OTUs in the Biomass and Solid samples. (B) Bar plot depicting the relative abundances at Genus level of the most abundant members of the Biomass and Solid samples. (C) Identity network showing the phylogenetic distance (edges) between the *Acidianus* spp. and *Sulfolobus* spp. reference and the reactor microbiome.

Declaration of Competing Interest

The authors declare that they have no known competing financial interests or personal relationships that could have appeared to influence the work reported in this paper.

Acknowledgements

We want to thank Victor J. Carrión and Javier Ramiro-Garcia for their valuable advice and support in the bioinformatics analysis.

This research was financially supported by a scholarship from CONICYT-Chile (grant number 72150546) granted to S.P Vega-Hernandez, the Dutch TKI program and Paques BV.

Appendix A. Supplementary data

Supplementary data to this article can be found online at https://doi.org/10.1016/j.cej.2020.127758.

References

[1] P. Riveros, J. Dutrizac, P. Spencer, Arsenic disposal practices in the metallurgical industry, Can. Metall. Q. 40 (2001) 395–420.
[2] A. Vahidnia, G.B. van der Voet, F.A. de Wolff, Arsenic neurotoxicity — A review, Hum. Exp. Toxicol. 26 (2007) 823–832.
[3] A. Wang, K. Zhou, X. Zhang, D. Zhou, C. Peng, W. Chen, Arsenic removal from highly-acidic wastewater with high arsenic content by copper-chloride synergistic reduction, Chemosphere 124675 (2019).
[4] N. Okibe, M. Koga, K. Sasaki, T. Hirajima, S. Heguri, S. Asano, Simultaneous oxidation and immobilization of arsenite from refinery waste water by thermoacidophilic iron-oxidizing archaeon, Acidianus brierleyi, Minerals Eng. 48 (2013) 126–134.
[5] Y. Jia, G.P. Demopoulos, Coprecipitation of arsenate with iron(III) in aqueous sulfate media: Effect of time, lime as base and co-ions on arsenic retention, Water Res. 42 (2008) 661–668.
[6] N.J. Welham, K.A. Malatt, S. Vukcevic, The stability of iron phases presently used for disposal from metallurgical systems—A review, Miner. Eng. 13 (2000) 911–931.
[7] D. Mohan, C.U. Pittman, Arsenic removal from water/wastewater using adsorbents—A critical review, J. Hazard. Mater. 142 (2007) 1–53.
[8] R.G. Robins, P.M. Dove, J.D. Rimstidt, D.K. Nordstrom, G.A. Parks, Solubility and stability of scorodite, FeAsO4·2H2O; discussions and replies, Am. Mineral. 72 (1987) 842–855.
[9] G.P. Demopoulos, On the preparation and stability of Scorodite, R.G. Reddy, V. Ramachandran (Eds.), Arsenic Metallurgy, TMS, Warrendale, PA (2005), (2005) 25-50.
[10] J. Dutrizac, J. Jambor, The synthesis of crystalline scorodite, FeAsO 4· 2H 2 O, Hydrometallurgy 19 (1988) 377–384.
[11] P. González-Contreras, J. Weijma, C.J.N. Buisman, Continuous bioscorodite crystallization in CSTRs for arsenic removal and disposal, Water Res. 46 (2012) 5883–5892.
[12] P. Gonzalez-Contreras, J. Weijma, R.V.D. Weijden, C.J.N. Buisman, Biogenic Scorodite Crystallization by Acidianus sulfidivorans for Arsenic Removal, Environ. Sci. Technol. 44 (2010) 675–680.
[13] N. Okibe, M. Koga, S. Morishita, M. Tanaka, S. Heguri, S. Asano, K. Sasaki, T. Hirajima, Microbial formation of crystalline scorodite for treatment of As (III)-bearing copper refinery process solution using Acidianus brierleyi, Hydrometallurgy 143 (2014) 34–41.
[14] M. Bissen, F.H. Frimmel, Arsenic — a Review. Part I: Occurrence, Toxicity, Speciation, Mobility, Acta hydrochimica et hydrobiologica 31 (2003) 9–18.
[15] B.K. Mandal, 7 - Changing Concept of Arsenic Toxicity with Development of Speciation Techniques, in: S.J.S. Flora (Ed.), Handbook of Arsenic Toxicology, Academic Press, Oxford, 2015, pp. 179–201.
[16] N. Higashidani, T. Kaneta, N. Takeyasu, S. Motomizu, N. Okibe, K. Sasaki, Speciation of arsenic in a thermoacidophilic iron-oxidizing archaeon, Acidianus brierleyi, and its culture medium by inductively coupled plasma–optical emission spectroscopy combined with flow injection pretreatment using an anion-exchange mini-column, Talanta 122 (2014) 240–245.
[17] B. Escobar, E. Huenupi, I. Godoy, J.V. Wiertz, Arsenic precipitation in the bioleaching of enargite by Sulfolobus BC at 70 °C, Biotechnol. Lett. 22 (2000) 205–209.
[18] E.B. Lindström, Å. Sandström, J.-E. Sundkvist, A sequential two-step process using moderately and extremely thermophilic cultures for biooxidation of refractory gold concentrates, Hydrometallurgy 71 (2003) 21–30.
[19] J. Ding, R. Zhang, Y. Yu, D. Jin, C. Liang, Y. Yi, W. Zhu, J. Xia, A novel acidophilic, thermophilic iron and sulfur-oxidizing archaeon isolated from a hot spring of tengchong, Yunnan, China, Braz. J. Microbiol. 42 (2011) 514–525.
[20] M. Tanaka, N. Okibe, Factors to Enable Crystallization of Environmentally Stable Bioscorodite from Dilute As(III)-Contaminated Waters, Minerals 8 (2018) 23.
[21] R. Debekaussen, D. Droppert, G.P. Demopoulos, Ambient pressure hydrometallurgical conversion of arsenic trioxide to crystalline scorodite, Anglais 94 (2001) 116–122.
[22] Y. Choi, A.G. Gharelar, N. Ahern, Method for arsenic oxidation and removal from process and waste solutions, Google Patents (2014).
[23] S. Vega-Hernandez, J. Weijma, C.J.N. Buisman, Immobilization of arsenic as scorodite by a thermoacidophilic mixed culture via As(III)-catalyzed oxidation with activated carbon, J. Hazard. Mater. 368 (2019) 221–227.
[24] S. Vega-Hernandez, J. Weijma, C.J.N. Buisman, Particle size control of biogenic scorodite during the GAC-catalysed As(III) oxidation for efficient arsenic removal in acid wastewaters, Water Resour. Ind. 23 (2020), 100128.
[25] U.S. EPA, Field Applications of In Situ Remediation Technologies: Chemical Oxidation, Washington D.C., EPA, 1998.
[26] D.M. van Vliet, S. Palakawong Na Ayudthaya, S. Diop, L. Villanueva, A.J.M. Stams, I. Sánchez-Andrea, Anaerobic Degradation of Sulfated Polysaccharides by Two Novel Kiritimatiellales Strains Isolated From Black Sea Sediment, Frontiers in Microbiology 10 (2019).
[27] R.C. Edgar, MUSCLE: a multiple sequence alignment method with reduced time and space complexity, BMC Bioinf. 5 (2004) 113.
[28] M.N. Price, P.S. Dehal, A.P. Arkin, FastTree: Computing Large Minimum Evolution Trees with Profiles instead of a Distance Matrix, Mol. Biol. Evol. 26 (2009) 1641–1650.
[29] I. Letunic, P. Bork, Interactive tree of life (iTOL) v3: an online tool for the display and annotation of phylogenetic and other trees, Nucleic Acids Res. 44 (2016) W242–W245.
[30] F. Sievers, Fast, scalable generation of high-quality protein multiple sequence alignments using Clustal Omega, Mol. Syst. Biol. 7 (2011) 539.
[31] P. Shannon, A. Markiel, O. Ozier, N.S. Baliga, J.T. Wang, D. Ramage, N. Amin, B. Schwikowski, T. Ideker, Cytoscape: A Software Environment for Integrated Models of Biomolecular Interaction Networks, Genome Res. 13 (2003) 2498–2504.
[32] T. Fujita, R. Taguchi, M. Abumiya, M. Matsumoto, E. Shibata, T. Nakamura, Effect of pH on atmospheric scorodite synthesis by oxidation of ferrous ions: Physical properties and stability of the scorodite, Hydrometallurgy 96 (2009) 189–198.
[33] D. Paktunc, J. Dutrizac, V. Gertsman, Synthesis and phase transformations involving scorodite, ferric arsenate and arsenical ferrihydrite: Implications for arsenic mobility, Geochim. Cosmochim. Acta 72 (2008) 2649–2672.
[34] S. Singhania, Q. Wang, D. Filippou, G.P. Demopoulos, Acidity, valency and third-ion effects on the precipitation of scorodite from mixed sulfate solutions under atmospheric-pressure conditions, Metallurgical and Materials Transactions B 37 (2006) 189–197.
[35] P.A. Gonzalez Contreras, Bioscorodite: biological crystallization of scorodite for arsenic removal, Wageningen university, [S.l.s.n.] (2012).
[36] A.M. Nazari, R. Radzinski, A. Ghahreman, Review of arsenic metallurgy: Treatment of arsenical minerals and the immobilization of arsenic, Hydrometallurgy 174 (2017) 258–281.
[37] R. Lakerveld, J.J.H. van Krochten, H.J.M. Kramer, An Air-Lift Crystallizer Can Suppress Secondary Nucleation at a Higher Supersaturation Compared to a Stirred Crystallizer, Cryst. Growth Des. 14 (2014) 3264–3275.
[38] C.T. Frijters, M. Silvius, J. Fischer, R. Haarhuis, R. Mulder, Full-scale applications for both COD and nutrient removal in a CIRCOX airlift reactor, Water science and technology : a journal of the International Association on Water, Pollution Research 55 (2007) 107–114.
[39] B.H.G.W. van Houten, K. Roest, V.A. Tzeneva, H. Dijkman, H. Smidt, A.J.M. Stams, Occurrence of methanogenesis during start-up of a full-scale synthesis gas-fed reactor treating sulfate and metal-rich wastewater, Water Res. 40 (2006) 553–560.
[40] Y. Jia, L. Xu, X. Wang, G.P. Demopoulos, Infrared spectroscopic and X-ray diffraction characterization of the nature of adsorbed arsenate on ferrihydrite, Geochim. Cosmochim. Acta 71 (2007) 1643–1654.
[41] S.J.S. Qazi, A.R. Rennie, J.K. Cockcroft, M. Vickers, Use of wide-angle X-ray diffraction to measure shape and size of dispersed colloidal particles, J. Colloid Interface Sci. 338 (2009) 105–110.
[42] J.W. Mullin, Crystallisation, 4th Edition American Chemical Society, Oxford, UK. , 2001.
[43] M.A. Gomez, H. Assaaoudi, L. Becze, J.N. Cutler, G.P. Demopoulos, Vibrational spectroscopy study of hydrothermally produced scorodite (FeAsO4·2H2O), ferric arsenate sub-hydrate (FAsH; FeAsO4·0.75H2O) and basic ferric arsenate sulfate (BFAS; Fe[(AsO4)1–x(SO4)x(OH)x]·wH2O), J. Raman Spectrosc. 41 (2010) 212–221.
[44] P. Gonzalez-Contreras, J. Weijma, C.J.N. Buisman, Bioscorodite Crystallization in an Airlift Reactor for Arsenic Removal, Cryst. Growth Des. 12 (2012) 2699–2706.
[45] Y. Sun, Q. Yao, X. Zhang, H. Yang, N. Li, Z. Zhang, Z. Hao, Insight into mineralizer modified and tailored scorodite crystal characteristics and leachability for arsenic-rich smelter wastewater stabilization, RSC Adv. 8 (2018) 19560–19569.
[46] T. Fujita, R. Taguchi, M. Abumiya, M. Matsumoto, E. Shibata, T. Nakamura, Novel atmospheric scorodite synthesis by oxidation of ferrous sulfate solution. Part II. Effect of temperature and air, Hydrometallurgy 90 (2008) 85–91.
[47] M.L. Caetano, V.S.T. Ciminelli, S.D.F. Rocha, M.C. Spitale, C.L. Caldeira, Batch and continuous precipitation of scorodite from dilute industrial solutions, Hydrometallurgy 95 (2009) 44–52.
[48] M.C. Harvey, M.E. Schreiber, J.D. Rimstidt, M.M. Griffith, Scorodite Dissolution Kinetics: Implications for Arsenic Release, Environ. Sci. Technol. 40 (2006) 6709–6714.
[49] A. Orell, S. Schopf, L. Randau, M. Vera, Biofilm Lifestyle of Thermophile and Acidophile Archaea, in: G. Witzany (Ed.), Biocommunication of Archaea, Springer International Publishing, Cham, 2017, pp. 133–146.

[50] D.E. Rawlings, D.B. Johnson, The microbiology of biomining: development and optimization of mineral-oxidizing microbial consortia, Microbiology 153 (2007) 315–324.
[51] D.B. Johnson, Biodiversity and interactions of acidophiles: Key to understanding and optimizing microbial processing of ores and concentrates, Trans. Nonferrous Metals Soc. China 18 (2008) 1367–1373.
[52] N. Okibe, S. Morishita, M. Tanaka, T. Hirajima, K. Sasaki, Effect of Cu (II) on Bio-Scorodite Crystallization Using Acidianus brierleyi, Adv. Mater. Res., Trans. Tech. Publ. (2015) 101–104.
[53] P. Gonzalez-Contreras, J. Weijma, C.J. Buisman, Kinetics of ferrous iron oxidation by batch and continuous cultures of thermoacidophilic Archaea at extremely low pH of 1.1–1.3, Appl. Microbiol. Biotechnol. 93 (2012) 1295–1303.
[54] C.M. Zammit, N. Cook, J. Brugger, C.L. Ciobanu, F. Reith, The future of biotechnology for gold exploration and processing, Miner. Eng. 32 (2012) 45–53.
[55] F. Battaglia-Brunet, M.C. Dictor, F. Garrido, C. Crouzet, D. Morin, K. Dekeyser, M. Clarens, P. Baranger, An arsenic(III)-oxidizing bacterial population: selection, characterization, and performance in reactors, J. Appl. Microbiol. 93 (2002) 656–667.
[56] M.F. DeFlaun, J.K. Fredrickson, H. Dong, S.M. Pfiffner, T.C. Onstott, D.L. Balkwill, S.H. Streger, E. Stackebrandt, S. Knoessen, E. van Heerden, Isolation and characterization of a Geobacillus thermoleovorans strain from an ultra-deep South African gold mine, Syst. Appl. Microbiol. 30 (2007) 152–164.
[57] P. Menzel, S.R. Gudbergsdóttir, A.G. Rike, L. Lin, Q. Zhang, P. Contursi, M. Moracci, J.K. Kristjansson, B. Bolduc, S. Gavrilov, N. Ravin, A. Mardanov, E. Bonch-Osmolovskaya, M. Young, A. Krogh, X. Peng, Comparative Metagenomics of Eight Geographically Remote Terrestrial Hot Springs, Microb. Ecol. 70 (2015) 411–424.
[58] J. Liu, Q. Li, W. Sand, R. Zhang, Influence of Sulfobacillus thermosulfidooxidans on Initial Attachment and Pyrite Leaching by Thermoacidophilic Archaeon Acidianus sp, DSM 29099, Minerals 6 (2016) 76.
[59] J.V. Wiertz, M. Mateo, B. Escobar, Mechanism of pyrite catalysis of As (III) oxidation in bioleaching solutions at 30 C and 70 C, Hydrometallurgy 83 (2006) 35–39.
[60] D.A. Clark, P.R. Norris, Oxidation of mineral sulphides by thermophilic microorganisms, Miner. Eng. 9 (1996) 1119–1125.